Flow Measurement and Instrumentation 55 (2017) 37–43

Contents lists available at ScienceDirect

Flow Measurement and Instrumentation

journal homepage: www.elsevier.com/locate/flowmeasinst

Temperature correlation velocimetry technique in liquid metals

I.A. Belyaev, N.G. Razuvanov, V.G. Sviridov, V.S. Zagorsky*

Joint Institute for High Temperatures of the Russian Academy of Sciences Moscow, Russia

ARTICLE INFO

Keywords:
Liquid metal
Temperature sensor
Temperature correlation velocimetery
TCV

ABSTRACT

The article describes the temperature cross-correlation velocimetry method applied to liquid metal flows. The technique allows to measure temperature waveforms and average longitudinal velocity in a flow simultaneously. The used micro thermocouple sensor and signal processing procedure are described in comparison with other works where the same or a similar approach have been implemented. Examples of experimental results obtained in MPEI[1] – JIHT[2] mercury facilities, are also provided. Method has been successfully used in magnetic fields up to 1 T.

1. Introduction

The local velocity measurement in liquid metal (LM) has been not an easy task since many difficulties have to be addressed. When choosing a measurement method, the following features of liquid metal should be taken into account:

1. High density;
2. High electrical and thermal conductivity;
3. Opacity;
4. High temperatures (except mercury, InGaSn, Na-K and some other alloys);
5. Toxicity;
6. Oxides and contaminants presence;
7. Chemical activity;
8. Electromagnetic issues.

A variety of techniques commonly used to measure flow velocity are not applicable at all or require significant modification to be used in liquid metal flow.

Invasive technique in liquid metal faces high demands on sensor's tightness and durability in conjunction with a reasonably small measuring point localization.

The possible velocimetry methods in relation to conducted research of mercury heat transfer and hydrodynamics in heated channels affected by magnetic field [1], have been considered. The goal is to obtain longitudinal velocity component profiles in the channel's cross section.

For quite a long time the temperature correlation velocimetry (TCV) had shown itself as one of the simplest and the most reliable among several common methods [2–4] used in MPEI and JIHT researches.

This method is intuitive; it appears naturally in environments with multiple points of temperature measurement [5,6]. Serious development was connected with researches dedicated to the nuclear industry [7–10] in 1970s. However, obtaining high-accurate results was time-consuming. The complexity and big amount of the equipment required for analog signal processing have become a significant barrier to widespread implementation at that time. In the cross-correlation technique, a significant role is given to flowmeters in which a special form of flow tract creates conditions convenient for steady flow measurement by the correlation method [11–13].

The TCV technique discussed herein is fundamentally similar to the approaches developed in the flowmeter solutions design though has significant distinctions. The main one is the desire to achieve complete absence of flow disturbance by the measuring sensor, as well as minimizing the base distance between the temperature sensors aimed at measurement localization. Examples of this approach are given in [14–16] and discussed below in comparison with our own results. It is necessary to emphasize the difference in cases when measurement points are separated by a significant distance [5,6,17]. In this case, the changes of flow itself should be considered (spatial averaging effect) which causes extra difficulties and is not discussed in this paper. There is no clear borderline between the flowmeter technique and more localized measurements. However, we categorized TCV separately as a technique able to measure local velocity using temperature waveforms without significant flow disturbance.

The TCV technique described in the article was used for velocity profile measurements in mercury flow in vertical, horizontal and

* Corresponding author.
E-mail addresses: bia@ihed.ras.ru (I.A. Belyaev), zagorskyvs@gmail.com (V.S. Zagorsky).
[1] *Moscow Power Engineering Institute*
[2] *Joint Institute for High Temperatures of the Russian Academy of Sciences*

http://dx.doi.org/10.1016/j.flowmeasinst.2017.05.004
Received 14 December 2015; Received in revised form 2 March 2017; Accepted 5 May 2017
Available online 06 May 2017

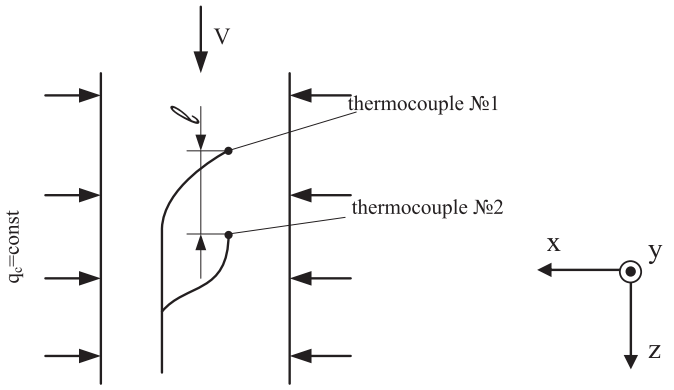

Fig. 1. TCV- basic scheme.

inclined channels affected by thermogravitation and strong magnetic fields of various orientation (transverse, longitudinal) [1].

2. Temperature correlation measurements

2.1. Sensor

To measure the temperature cross-correlation with subsequent achieving the longitudinal velocity component V_z, the authors used a sensor with basics shown in Fig. 1. It consists of two micro thermocouples (in our case type – T) with a fixed distance between them. Thermocouples junction probe is located on the centerline. The actual sensor views are shown in Fig. 2.

Thermocouple hot junction size was $\delta = 0{,}2$ mm, the distance between thermocouples in most of our experiments was $l = 5{,}0$ mm for velocities ranging 1–250 mm/s, and with heat flux q_c through the tube wall. Thermocouples were attached to steel capillaries with high temperature epoxy adhesive. The sensor was mounted on the end of a swivel-type probe (Fig. 3).

Some probe measurements were performed with the longitudinal magnetic field presence. This could have an impact on sensor readings associated with conductive fluid flow deceleration in magnetic field. This creates a so-called "front wake" [18]: flow distortion caused by sensor extended in the upstream. The typical size δ_p of the perturbation region in the direction of the average velocity is taken as $\delta_p/d_T = N_T^{0.5}$ [19], where $N_T = \frac{Ha^2}{\mathrm{Re}}$ is a local Stuart number (local MHD parameter) calculated using streamlined body diameter d_T. as a characteristic length. In our case, magnetic induction was up to B = 1T. This fact had been considered in the probes design.

The probe size ratio was chosen in such a way so that probe elements "front track" did not reach the neighboring microthermocouples. Besides, the work [20] has been taken into account and resulted in conclusion that the cylindrical body in a longitudinal magnetic field flowed round about substantially the same as in its absence if $N_T \leq 0,7$. In most of our experiments this inequality was correct up to B = 0.5 T which gave us less than 1 mm front track.

The above measurement difficulties in liquid metal flows are partly compensated by the following favorable features of temperature fields of liquid metals. Due to the high thermal conductivity the average temperature, profiles and temperature fluctuations statistical characteristics in the flow vary quite smoothly even near the heated wall. Thus, measurements in the mercury flow do not have such high requirements for the thermocouple junction's size and setting coordinates accuracy, as compared, for example, to measurements performed in a water flow. When using the probe, especially when dealing with complex multi thermocouple probes for dimensional correlation functions research, we have to put up with the inevitable small-scale perturbations of the velocity field. However, in liquid metals these perturbations do not affect the temperature field structure. This happens since only relatively large thermal inhomogeneities may exist in liquid metals, while smaller ones are absorbed due to high molecular thermal conductivity. Indeed, in a non-isothermal isotropic turbulence we have the following ratio between the Taylor microscales for velocity λ_V and temperature λ_T fluctuations:

$$\lambda_V/\lambda_T = \sqrt{\mathrm{Pr}}\,.$$

Taylor time microscales can be found from autocorrelation function of a signal sample:

$$\frac{1}{\lambda^2} = -\frac{1}{2}\left(\frac{\partial^2 R_{xx}(\tau)}{\partial \tau^2}\right)_{\tau=0},$$

where R_{xx}- autocorrelation function.

Our correlation measurements show that time microscales and therefore sizes of temperature fluctuations during our experiments in mercury flow are quite large – sizes are about several millimeters. This confirms our conclusion about the low sensitivity of the temperature field in the liquid metal to the local small-scale velocity perturbations.

The swivel-type probe is basically a rod pivotally mounted on the frame. The probe moves by rotating the cross-pivot caliper screw attached to the end of the probe rod. Movement is controlled by indicators. Each movement is followed with a pause in measurements to stabilize the flow. The probe's natural frequencies are higher than observed in hydrodynamics air, water, and mercury flow measurements by several orders. The probe positioning in the channel section is ensured by defining the wall touch along the temperature profile fracture (Fig. 4).

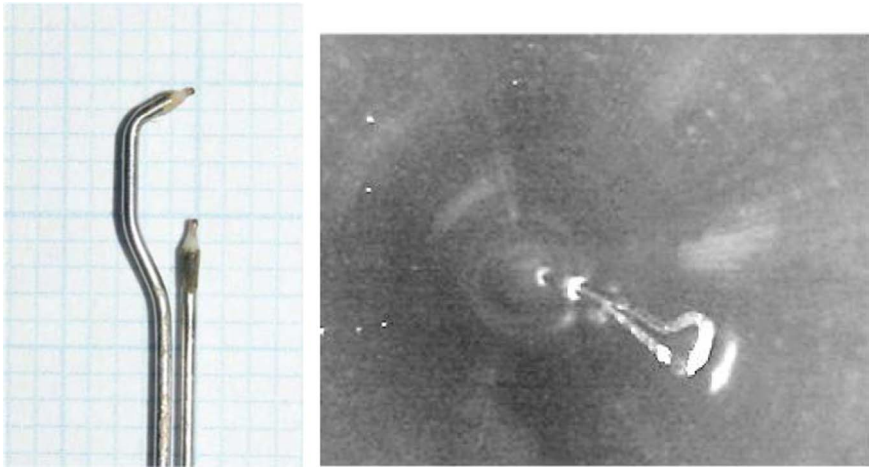

Fig. 2. TCV – sensor: side view and front view inside a tube (19 mm inner diameter).

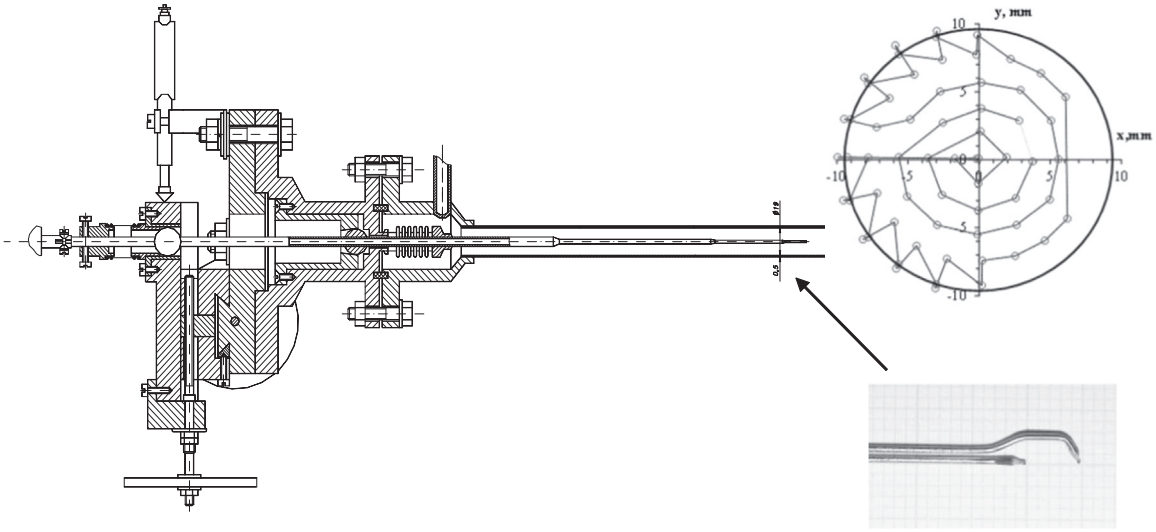

Fig. 3. Swivel – type probe, TCV sensor, and typical measurement points mapped in the tube's cross-section.

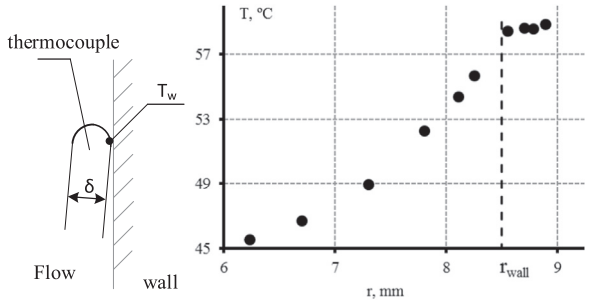

Fig. 4. Wall defining by temperature profile fracture.

Velocity profiles are measured by the temperature waveform processing from both thermocouples using natural turbulent temperature fluctuations background. Velocity measurement is carried out principally in the core flow. This was made as Taylor's frozen-flow hypothesis [21] of "frozen" turbulence (underlying the basis of TCV method) loses its effect near the wall.

Simultaneous measurement of the front and the rear thermocouples is shown in Fig. 5.

2.2. Processing procedure

If l is the distance between thermocouples and τ_T is a signal delay from the second thermocouple averaged over the time, then the local velocity value V_z can be easily calculated:

$$V_z = \frac{l}{\tau_T} \tag{1}$$

In the TCV method, the time delay corresponds to the maximum coordinate on the cross-correlation function (CCF). Theoretically, CCF for two stationary random centered signals X(τ) and Y(τ) is given by:

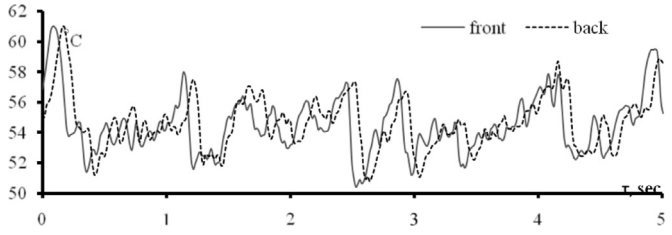

Fig. 5. Temperature waveforms sample, $V_0 = 0.06$ m/s, $q = 35$ kW/m^2 obtained by TCV sensor in flow core.

$$R_{XY}(S) = \frac{1}{\sigma_X \sigma_Y} \lim_{t \to \infty} \frac{1}{t} \int_0^t X(\tau) Y(\tau + S) d\tau, \tag{2}$$

where S is a time shift, τ is a current process time, t is time averaging, σ is a standard deviation. To estimate the delay time, it is sufficient to have information on the small-scale structure of the turbulent flow temperature background.

Practically used limited-time implementation of the X (τ) = T_1 (τ) and Y (τ) = T_2 (τ), where T_1 (τ) and T_2 (τ) are centered signals from thermocouples number 1 and number 2 of the TCV sensor. In fact, CCF R_{12} of thermocouples signal correlation was determined with the following formula:

$$R_{12}(s) = \frac{1}{N} \sum_{i=1}^{N} \frac{T_1(i\Delta\tau) T_2(i\Delta\tau + s)}{\sigma_X \sigma_Y}, \tag{3}$$

where s is a CCF parameter, time shift $s = j \cdot \Delta\tau$ ($j = 0, 1, \ldots$); $\Delta\tau$ is a time step determined by sampling a frequency of the measuring device; N is a sample size.

Waveforms example obtained by TCV sensor's thermocouples is shown in Fig. 5. It is evident that the signal from thermocouple #2 repeats signal #1 with a certain delay. The τ_T delay is determined by the CCF maximum coordinate (s_{max}). Fig. 6 shows a normalized CCF example achieved with different distance between thermocouples – l. These results were measured using specialized probe which allowed moving rear thermocouple and thus changing the distance between thermocouples within the same experimental conditions. It is obvious that at $l = 0$ (first curve) the CCF turns into autocorrelation function.

On the one side, we should have the distance - l as small as possible

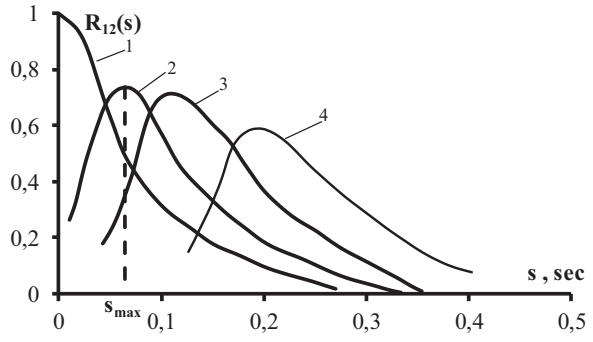

Fig. 6. CCF functions of sensors with different distances between thermocouples (l), 1 - $l = 0$; 2 – $l = 2$ mm; 3 – $l = 5$ mm; 4 – $l = 10$ mm. $Re = 10^4$ ($V_0 = 0.06$ m/s), without magnetic field, sensor is placed in the middle of the tube radius (R = 0.5).

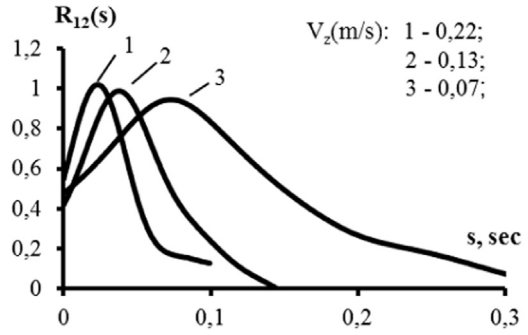

Fig. 7. CCF functions of sensor with fixed distance between thermocouples $l = 5$ mm at different velocities.

to minimize localization point of velocity value and make the sensor more compact and, therefore, more durable. On the other, if l is too small, it is difficult to achieve a good CCF maximum in a wide velocities range.

The influence of geometric, thermal, and hydrodynamic factors of a sensor on TCV measurement quality and stability is complicated. Considering this, the dimensionless complex K has been proposed for experimental data generalization in the experiments [10]. K is basically a ratio between the thermocouple inertia (τ_α) and expected average delay time between thermocouple signals (l/V_z):

$$K = \tau_\alpha \frac{V_z}{l}, \tag{4}$$

Based on water experiments [10] the common recommendation is to be in range of 0.1–1 has been given for parameter K. In our further experiments, $l = 5$ mm was used. CCF results achieved at different velocities using sensor with fixed distance between thermocouples are shown in Fig. 7. In our case, we had K ranged 0.03–1 still having a nice CCF maximum. In works [15,16] the sampling rate is used to define K-similar recommendations. In our opinion, this is not correct since sampling rate may vary within very wide limits depending on current data acquisition system.

In our work, measurements and tests were carried out in the experimental magneto-hydrodynamic (MHD) facilities of MPEI-JIHT RAS [1,22]. The experiment was mostly automated using modern hardware and software. In particular, our probe measurements were made using two 4071 digital multimeters produced by National Instruments.

Sampling rate was not less than 2000 samples per second, a step time of 0.5 ms. For signal post processing we used waveforms of 20 − 120 s length. In principle, sampling rate should only be twice more than observed in process due to Nyquist sampling criterion. Multispeed digitizing was used to implement digital low pass filters, which were necessary to avoid electrical noises from power grid and other sources.

TCV technique provides data about mean longitudinal velocity and temperature waveform simultaneously, this is useful in performing thermophysical experiment.

2.3. Calibration

The sensor calibration was made as follows: sensor was installed in the 19 mm inner diameter tube's center, after ~77 calibers of stabilization. Measured data were compared with value calculated from the flow rate using the Reichardt [23] equations:

$$V_z = \varphi \cdot u^*;$$

$$\varphi(\eta) = 2.5 \ln(1 + 0.4\eta) + 7,\ 8\left(-e^{-\eta/11} - \frac{\eta}{11} e^{-0.33\eta}\right);$$

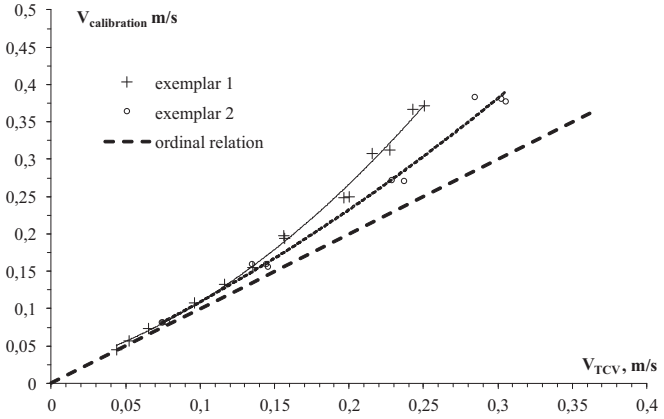

Fig. 8. TCV – sensor calibration.

$$u^* = \overline{V}\sqrt{\frac{\xi}{8}};$$

$$\eta = y \cdot u^*/\nu,$$

where φ – is a dimensionless velocity, u*– dynamic velocity, ξ – hydraulic friction coefficient, $\overline{V}$ – average velocity, η –dimensionless distance from the wall, y – distance from the wall, ν – kinematic viscosity of liquid.

Flowrate was measured using Venturi tube calibrated on water having flow coefficient determined with 2% accuracy [24]. While calibrating, a small heat flux was used in such a way that temperature fluctuations were resenting but the flow deformation caused by thermo gravitation was not sufficient (recommendations from [25] used). Presented as a diagram (Fig. 8), the data shows that the measured values are lower than velocity calculated from the flow rate by Reichard formula. Two different handmade exemplars of a TCV sensor are presented, both showing similar calibration dependencies. The difference lies in geometrical divergence. Further, we present results gathered using individual calibration by these and other sensors without specifying the used sensor.

This may be explained by the problem typical for all invasive probes: first thermocouple in the fluid flow creates the flow disturbance. Therefore, the mean velocity between thermocouples is lower than that in the undisturbed area. Moreover, this disturbance increases with respect to the flow velocity. The 3rd-order polynomial function is enough to describe the needed correction. One shot measurement shows 7% maximum deviation from calibration function. This result is compatible with ± (5 − 10)% accuracy achieved in [15,16].

Also, one can see that no correction is needed up to velocity 0.1 m/s in mercury. This aspect should be stressed. No calibration is needed to use the described TCV methodic up to a certain velocity. Beyond it, the maximum deviation from ordinal relation is 26% at a velocity of 0.38 m/s for 2%, and 34% at velocity 0.37 m/s.

This fact is a significant advantage of the proposed method when used in industrial applications, since reasonable precision can be obtained without any calibration.

3. Examples of experimental results

The example of the longitudinal velocity distribution along the 19 mm tube cross-section is shown in a dimensionless form in Fig. 9. The mean velocity in a tube V_o is used as a scale factor. In the above example it was impossible to achieve data in the area $R > 0.8$ using the TCV sensor due to limitations originating from the sensor's construction size and false correlations in a "near-wall region".

Fig. 10 shows velocity distribution over tube radius achieved in the whole cross section. In this particular experiment temperature fluctuation intensity was in a range 0.03–0.05 °C. Changes in sensor orienta-

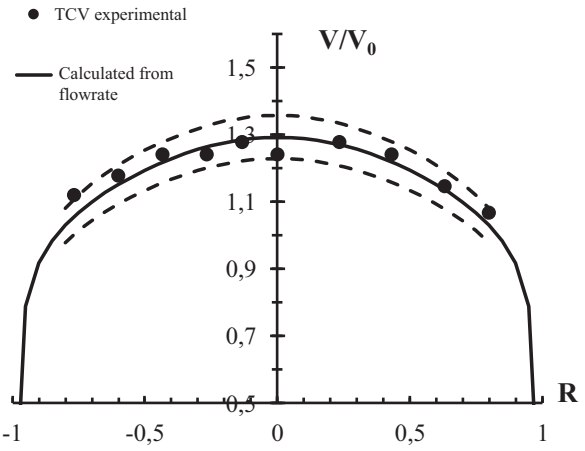

Fig. 9. Dimensionless longitudinal velocity distribution over tube diameter, mean velocity – $V_0 = 0.12$ m/s, heating $q = 5$ kW/m^2, Dashed line shows 5% deviation from flowrate calculated velocity.

tion inside the channel caused by swivel probe construction resulted in changes of flow disturbance pattern captured by the sensor's front thermocouple. The measurements of articulated probe cause radial displacement of the thermocouples not exceeding 0.3 mm, and, apparently, not having a significant impact on the measurement beyond random inaccuracy. This result is consistent with the work [10] where the displacement from channel axis up to 30% of the basic distance was found not to affect the measurement results.

That worst measurements during calibration was found aside the tube center in $R > 0.8$ area. However, in [16] a successful measurement near the wall including the viscous sublayer had been done. Thus, we have encountered difficulties which are plausibly related to the rather massive sensor size.

Some examples of experimental dimensionless longitudinal velocity fields obtained with TCV compared to numerical simulations [26] are shown in Fig. 11. For the purposes of convenience, the experimental data obtained with the sensor is supplemented with null values on the wall and is reflected in the horizontal plane due to expected symmetry of the result.

A significant uniform heat flow, $q = 35$ kW/m^2, in a horizontal tube developed a secondary flow of thermo gravitational convection (TGC), which had the two symmetrical longitudinal vortices formed. TGC is superimposed on the main flow and deforms the latter, breaking the axial symmetry of the turbulent velocity field. The maximum velocity is shifted towards the tube's bottom. Contours built by experimental and numerical data almost coincide revealing the TCV technique applicability in the presence of secondary flows.

The correlation method is a direct method for velocity measurements, so it can be applied for straight and reverse flows. The probe causes additional non-compensated disturbances to measurements in the reverse flow case. The example of such measurements obtained in inclined tubes [27] is shown in Fig. 12. Longitudinal velocity deformations under longitudinal magnetic field (MF) influence are presented. Thermogravitation force influence resulted in inhibited zone development at top of the tube ($R > 0$), and longitudinal MF caused a successive reverse flow emergence. The TCV method did provide us with a possibility to measure the whole profile, areas of transition from reverse to straight flow are unavailable. However, we assume that the fact of return flow presence is evident, but the region and negative velocity values are defined only qualitatively.

Measurements were successfully made in velocity range of 0.02–0.3 m/s at longitudinal magnetic fields of up to 1 T. However, careful interpretation is needed in case induction is higher than 0.5 T, as flow might be disturbed by the "front track" sensor described above.

Experiments in transverse magnetic field were also conducted. Transverse MF suppress velocity fluctuation much stronger than longitudinal and, therefore, temperature fluctuation intensity and spectrum density is either suppressed. This fact makes it difficult to implement TCV technique as it is based on natural turbulence fluctuations background. However, large flow structures revealing themselves in case of TGC and MF joint influence create conditions where TCV measurements application is possible [28,29].

As an example, dimensionless velocity profiles are shown in Fig. 13. Measurements were conducted in a one side-heated duct [28]. The $X = x/b$ axis is directed along the large side of the duct cross section parallel to the MF. The probe could reach the middle of the channel in this direction, the inaccessible part for the ease of reference is given in the form of a symmetrical reflection of the received data (Fig. 13a).

The velocity distributions along X axis are uniform (Fig. 13a). These profiles are flattened with magnetic field induction increasing according to Hartmann effect. The velocity distributions along the short duct side (axis $Y = y/b$) do not have side wall jets due to electro insulating layer presence, but demonstrate strong buoyancy influence (Fig. 13b).

Experiments with transverse MF where made in 0,02–0.5 m/s velocity range in magnetic fields of up to 1 T. The TCV method applicability depends on the channel geometry, heating embodiment, and the value of magnetic induction. Common usage recommendations in a transverse MF was not developed since transverse MF suppresses turbulent fluctuations in a more offensive manner as compared to the longitudinal one. In such situation, in most of our experiments the ordinary isothermal turbulence was suppressed, and some other flow perturbations are necessary for technique implementation which are not connected with sensor construction.

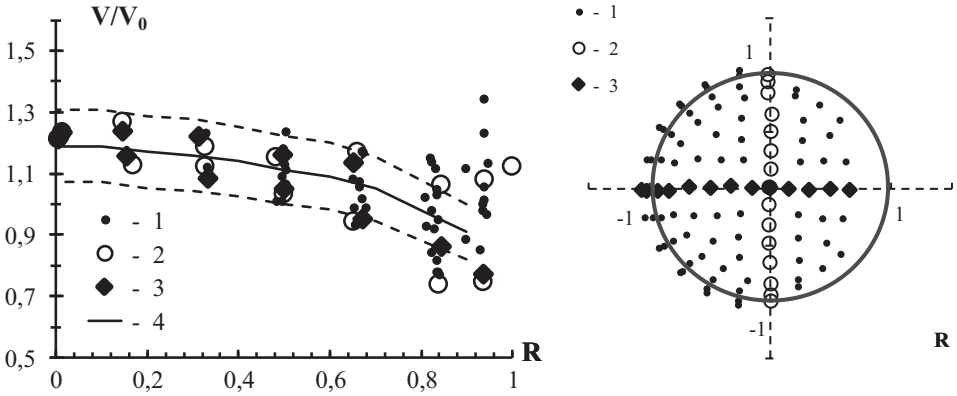

Fig. 10. Dimensionless longitudinal velocity distribution over tube radius, and tube cross section with measurement point location. Mean velocity $-V_0 = 0.27$ m/s, heating $q = 1$ kW/m^2: 1 – measurements in the tube cross section, 2 – vertical velocity profile, 3 – horizontal velocity profile, 4 – velocity calculated from flowrate; Dashed line shows 10% deviation from flowrate calculated velocity distribution.

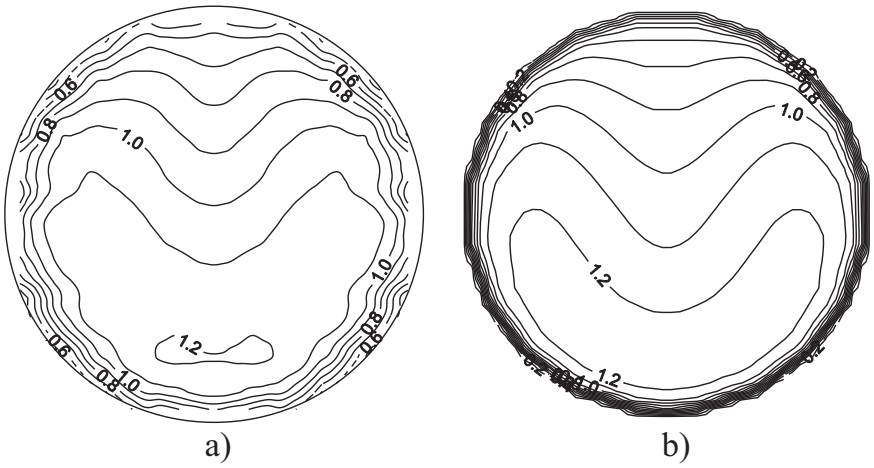

Fig. 11. Dimensionless longitudinal velocity field, mean velocity -V_0 = 0.06 m/s, Horizontal tube, uniform heating q = 35 kW/m^2: a) experiment, b) numerical simulation [26].

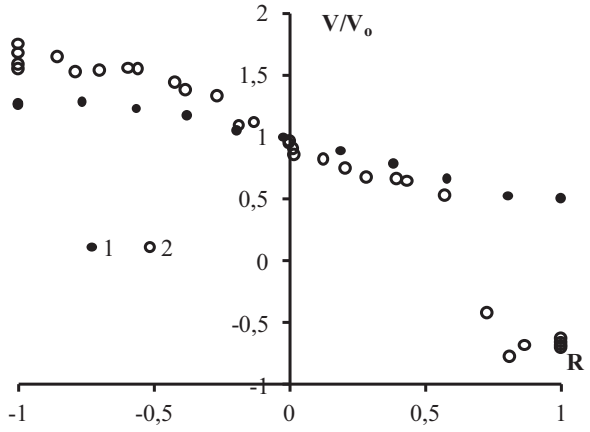

Fig. 12. Dimensionless longitudinal velocity profile over tube vertical cross-section (R = 1 – top, R = −1 bottom), mean velocity -V_0 = 0.06 m/s, inclined tube θ = 30° to horizon, uniform heating q = 35 kW/m^2, longitudinal magnetic field 1) B = 0 T, 2) B = 0.7 T.

4. Discussion

The described technique is based on digital signal processing obtained through the multi-speed digitizing method. In fact, the information sufficient to achieve the best possible result in determining the rate contained in the field and the hydrodynamic frequencies a) exist in the flow b) can be measured by a sensor having satisfactory inertness. The discreteness of the obtained CCF values may seem to be a hindrance, yet it can be restored in a unique manner if signal digitized with the frequency twice higher than that determined by the flow nature. Thus, when considering the *K*-similar parameter, it is recommended to take the actually observed width of the spectrum of temperature fluctuation as the time scale of the process. As for identification of the spectrum wideness, the inverse of the Taylor microscale is a great example. Such information can be obtained from studies on the statistical fluctuations temperature or direct measurements of single-point temperature sensors.

In measurements made in liquid metals, temperature sensors have a substantially lower inertia which allows even relatively massive sensors to confidently reproduce the entire width of the observed spectrum of temperature pulsations. The low viscosity of mercury also contributes to a more developed turbulence at comparable velocities. These aspects of TCV techniques for liquid metals cause even greater ease of implementation than, for example, for water. Seeming difficulties associated with blurring temperature track caused by higher values of the molecular conductivity only lead to a fold reduction of the temperature fluctuation [8] requiring a larger supply ratio of signal/noise. This might be easily overcome by using modern measuring tools.

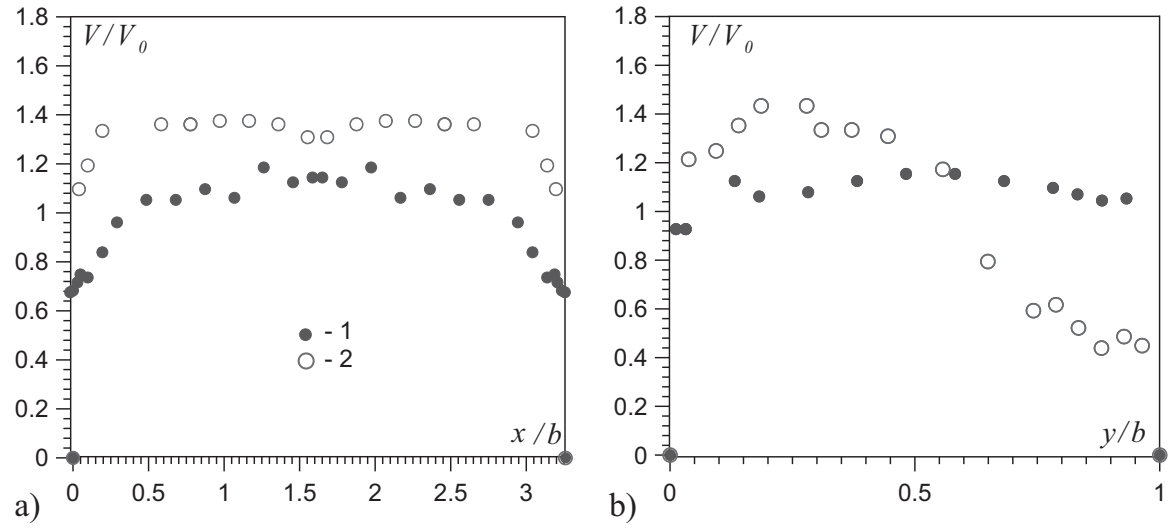

Fig. 13. The dimensionless longitudinal velocity distributions along X(Y = 0.5) (a) and Y(X = 1.6) (b) axes in the duct 20d cross section q_1 = 35 kW/m^2, V_0 = 0,17 m/s: 1) B = 0; 2) B = 0.86 T;.

5. Conclusion

Considering the described TCV features, the method proved itself as a highly convenient, providing the ability to perform complex measurements using the same sensor type. This fact is a significant advantage of the proposed method when using in industrial applications, since reasonable precision can be obtained without any calibration. Recommendations for selection of sensor parameters are based on our experience. Explored limits of applicability are defined. Examples of application in longitudinal and transverse magnetic fields are also shown.

Source of funding

Work is supported by RSCF project no. 14–50-00124.

References

[1] I.A. Belyaev, et al. Specific Features of Liquid Metal Heat Transfer in a Tokamak Reactor //Magnetohydrodynamics (0024-998X). –. T. 49, 2013.
[2] V.G. Zhilin, et al., Diagnostics of Liquid Metal Flows Using Fibre-optic Velocity Sensor/Liquid Metal Magnetohydrodynamics, Kluwer Academic, Dordrecht, 1989, pp. 373–379.
[3] R. Ricou, C. Vives, Local velocity and mass transfer measurements in molten metals using an incorporated magnet probe, Int. J. Heat. Mass Transf. (1982) 1579–1588.
[4] D.J. Malcolm, Hot-wire measurements is stationary magnetohydrodynamic flows of liquid metal using a platinum sensors, Magnetohydrodynamics 2 (1970) 55–64 (Electromagnetic sensor).
[5] S. Horanyi, L. Krebs, U. Müller, Turbulent Rayleigh–Bénard convection in low Prandtl–number fluids, Int. J. Heat. Mass Transf. 42 (21) (1999) 3983–4003.
[6] P. Frick, R. Khalilov, I. Kolesnichenko, A. Mamykin, V. Pakholkov, A. Pavlinov, S. Rogozhkin, Turbulent convective heat transfer in a long cylinder with liquid sodium, EPL (Europhys. Lett.) 109 (1) (2015) 14002.
[7] J. Benkert, C. Mika, K.H. Raes, D. Stegemann, Determination of thermocouple transfer-functions and fluid-flow velocities by temperature-noise measurements in liquid sodium, Prog. Nucl. Energy 1 (2) (1977) 553–563.
[8] R.L. Randall, Transit Time Flowmeter Employing Noise Analysis Techniques: Part 1.Water Loop Tests, Atomics International, Canoga Park, Calif, 1969.
[9] K.P. Termaat, Fluid flow measurements inside the reactor vessel of the 50 MWe Dodewaard nuclear power plant by cross-correlation of thermocouple signals, J. Phys. E: Sci. Instrum. 3 (8) (1970) 589.
[10] V.M. Selivanov, A.D. Martynov, V.S. Severyanov, A.P. Solopov, V.I. Sharypina, Institute of Physics and Power Engineering, Obninsk, USSR; D. Pallagi, Sh Horani, T.Haragitai, Sh.Tezher, Central Institute for Physical Research, Budapest, Hungary. Flow measurement by the correlation of random thermocouple signals in the circuits with natural circulation of the coolant. KFKI - 76 - 21 ISBN 963 371 123 1 (In Russian).
[11] B.V. Kebadze, Analysis of the statistical error and optimization of correlation flow meters, At. Energy 56 (1) (1984) 13–18.
[12] M.S. Beck, Correlation in instruments: cross correlation flowmeters, J. Phys. E: Sci. Instrum. (1981) (– T. 14. – №. 1. – C. 7).
[13] J. Coulthard, Cross-correlation flow measurement—a history and the state of the art, Meas. Control (1983) 214–218.
[14] S.R. Rockwell, An Investigation into the Use of Cross Correlation Velocimetry (Doctoral Dissertation), Worcester Polytechnic Institute, 2009.
[15] V. Motevalli, C.H. Marks, B.J. McCaffrey, Cross-correlation velocimetry for measurement of velocity and temperature profiles in low-speed, turbulent, non-isothermal flows, J. Heat. Transf. 114 (2) (1992) 331–337.
[16] T. Delarochelambert, Heat transfer and turbulence measurements in high temperature natural convection boundary layers using a single thermoanemometric probe. in: Proceedings of the 3rd European Thermal Sciences Conference, 2000, pp. 675–680.
[17] X.L. Qiu, P. Tong, Onset of coherent oscillations in turbulent Rayleigh-Bénard convection, Phys. Rev. Lett. (2001) 094501.
[18] J.A. Shercliff, Textbook of magnetohydrodynamics, 1965.
[19] M. Lake Bruce, Measurements of velocity before body moving through conducting fluid parallel to magnetic field, J. Fluid Mech. 50 (1971) 209–231.
[20] N.N. Polyakov, Calibration of Pitot tubes in a longitudinal magnetic field// V. KN.: in: Proceedings of the Tenth Riga conference on magnetic hydrodynamics. Vol. 1. Riga.: Znanie. S. 113 (In Russian), 1981.
[21] G.I. Taylor, Proc. R. Soc. Lond., Ser. A, 164, pp. 1938–476.
[22] H. Reichardt, Vollstflndige Darstellung der turbulenten Geschwindig-keitsverteilung in glatten Leitungen, ZAMM 31 (1951) 208–219.
[23] V.M. Batenin, et al., Modernization of the experimental base for studies of MHD heat exchange at advanced nuclear power facilities, High Temp. (2015) 904–907.
[24] N.G. Razuvanov, Study of MHD Heat Transfer in the Flow of Liquid Metal in a Horizontal Tube (Doctoral Dissertation), MPEI, Mosc. (2011) (In Russian).
[25] Ya.I. Listratov, D. Ognerubov, E.V. Sviridov, O. Zikanov, V.G. Sviridov, Direct numerical simulation of heat transfer and convection in mhd liquid metal flow in a pipe, Magnetohydrodynamics 49 (1–2) (2013) 87–100.
[26] V.G. Sviridov, et al. Liquid metal heat transfer investigations applied to tokamak reactor, in: Proceedings of the 14th International Heat Transfer Conference – American Society of Mechanical Engineers. 2010, 287-294.
[27] I.A. Belyaev, N.G. Razuvanov, V.G. Sviridov, V.S. Zagorsky, Liquid metal downflow in an inclined heated tube affected by longitudinal magnetic field, Magnetohydrodynamics 51 (4) (2015).
[28] I.R. Kirillov, et al., Buoyancy effects in vertical rectangular duct with coplanar magnetic field and single sided heat load, Fusion Eng. Des. (2016) 1–8.
[29] I.A. Belyaev, et al., Temperature fluctuations in a liquid metal MHD-flow in a horizontal inhomogeneously heated tube, High Temp. 53.5 (2015) 734–741.